

# Evolutionary Generative Adversarial Networks based on New Fitness Function and Generic Crossover Operator

Junjie Li, Jingyao Li, Wenbo Zhou, and Shuai Lü

**Abstract**—Evolutionary generative adversarial networks (E-GAN) attempts to alleviate mode collapse and vanishing gradient that plague generative adversarial networks by introducing evolutionary computation. However, E-GAN lacks a reasonable evaluation mechanism, which limits its effect. Moreover, E-GAN only contains mutation operators in its evolutionary step, while ignoring crossover operators. The crossover operator generates more competitive individuals by combining the good traits of multiple individuals, thus it can complement the mutation operator. In this paper, we propose a novel evolutionary generative adversarial networks framework called improved evolutionary generative adversarial networks (IE-GAN), which introduces a new fitness function and generic crossover operator. A more efficient fitness function can measure the evolutionary degree of individuals more precisely. And with the help of knowledge distillation, crossover offspring can learn knowledge from multiple networks simultaneously. Experiments on various datasets demonstrate the effectiveness of IE-GAN, and show that our framework is competitive in terms of the quality of generated samples and time efficiency.

**Index Terms**—Deep generative models, evolutionary strategy, generative adversarial networks, knowledge distillation.

## I. INTRODUCTION

GENERATIVE adversarial networks (GAN) [1] is a deep learning model and one of the most promising unsupervised learning methods in recent years. However, the training of GAN is challenging, and problems such as mode collapse and vanishing gradient are common [2]. To solve these problems, evolutionary computation has been introduced. As one of the most important evolutionary objects, a population consists of multiple individuals. A single individual encoded as genotype represents a neural network in an abstract way. Specifically, there are many different types of encoded genes, such as network structure and weights. The genotype is bijectively mapped to the phenotype of the individual, which represents a concrete neural network. The choice of individuals is based on the evaluation of the phenotype to produce a

better solution for the next generation. In this paper, we refer to the combination of GAN and evolutionary computation as evolutionary GAN.

Evolutionary generative adversarial networks (E-GAN) [3] is a concrete evolutionary GAN and it maintains a generator population that generates individuals with different loss functions as mutation operators. In each evolutionary step, individuals are evaluated in terms of quality and diversity. There are many researches that have improved E-GAN. For example, cooperative dual evolution based GAN (CDE-GAN) expands the concept of population to discriminator and uses a soft mechanism to connect the two populations [4]. Mu *et al.* define a novel mutation operator, i.e., a distribution indicating realness [5]. Multiobjective evolutionary GAN (MO-EGAN) considers quality and diversity as conflicting objectives, and defines the evaluation of generators as a multiobjective problem [6]. Mustangs is inspired by E-GAN and applies different loss functions to competitive co-evolutionary algorithm [7]. In addition to the E-GAN-based methods, there are many other studies on evolutionary GAN [8]–[12]. Nevertheless, each of these methods is weak in terms of crossover operator or individual evaluation.

In evolutionary computation, there are two common but crucial variation operators, i.e., mutation and crossover. The mutation operator produces new traits, and the crossover operator is used to combine the best traits of multiple individuals. However, evolutionary GAN rarely use the crossover operator. Although Garciarena *et al.* apply the crossover operator in [12], the crossover operator they used is difficult to transfer to other methods.

In addition, how to measure the diversity of the generated samples is also a controversial problem. Fréchet Inception Distance (FID) [13] is a model generation performance metric. It can reflect sample diversity, but requires a lot of time and space. And the resource consumption should not be neglected when FID is directly involved in the training process. E-GAN proposes a discriminator-based diversity metric, however, our experiments show that it is not as effective as expected.

The contributions of this paper are as follows:

- We analyze and experimentally verify the imperfection of E-GAN.
- We propose a generic backpropagation-based crossover operator, which can be applied to GANs with multiple generators regardless of specific model implementations.
- We propose a concise and effective diversity metric that can objectively reflect the diversity of the generated

Manuscript received August 7, 2021. This work was supported by the Natural Science Research Foundation of Jilin Province of China under Grant No. 20180101053JC; the National Key R&D Program of China under Grant No. 2017YFB1003103; and the National Natural Science Foundation of China under Grant No. 61300049. (*Corresponding author: Shuai Lü.*)

Junjie Li, Jingyao Li, and Shuai Lü are with the Key Laboratory of Symbolic Computation and Knowledge Engineering (Jilin University), Ministry of Education, China; College of Computer Science and Technology, Jilin University, China (e-mail: junjiel18@mails.jlu.edu.cn; jingyao18@mails.jlu.edu.cn; lus@jlu.edu.cn).

Wenbo Zhou is with the School of Information Science and Technology, Northeast Normal University, China (e-mail: zhouwb17@mails.jlu.edu.cn).

samples at a low cost.

- We design and implement a framework called improved evolutionary generative adversarial networks (IE-GAN) with our crossover operator and fitness function.

## II. RELATED WORKS

### A. E-GAN

E-GAN designs an adversarial framework between a discriminator and a population of generators [3]. Specifically, it assumes that the generators no longer exist as individuals, but as a population to confront with discriminator. From an evolutionary point of view, the discriminator can be considered as a changing environment during the evolutionary process.

In each evolutionary step of E-GAN, the evolution of the generator consists of three steps: variation, evaluation, and selection. The variation includes only mutation operation, and different loss functions are chosen as mutation operators to produce different offspring. Then, the generative performance of the generated offspring needs to be evaluated and quantified as the corresponding fitness. We will cite the fitness function in [3] as  $F^{E-GAN}$  in this paper to avoid confusion. After measuring the generative performance of all offspring, according to the principle of survival of the fittest, the updated generators are selected as the parents for a new round of training.

We proposed E-GAN with crossover (CE-GAN) in [14], which is the preliminary step of this work.

### B. Knowledge Distillation

Knowledge distillation is a model compression method, also a training method based on the “teacher-student network”, in which the knowledge contained in a trained model is distilled and applied to the target model. The target model is often a smaller model that is compressed and has better generalizability. The target model can learn to match any layer of the trained model. Hard targets mean learning with the output, which reduces training time, but increases the possibility of overfitting. Whereas soft targets learn from logits, which contain more descriptive information about the samples, and enable the target network to have better generalization capability [15].

As a means of compressing networks, knowledge distillation has been applied to GAN [16], [17]. Proximal distilled evolutionary reinforcement learning (PDERL) [18] utilizes this technique to optimize evolutionary reinforcement learning (ERL) [19]. It proposes a backpropagation-based crossover operator named  $Q$ -filtered behaviour distillation crossover. The experiments demonstrate that in reinforcement learning (RL), the operator can ensure that offspring inherit the behaviour of their parents. Thus,  $Q$ -filtered behaviour distillation crossover will not cause destructive interference like  $n$ -point crossover. Moreover,  $Q$ -filtered behaviour distillation crossover as a learning-based variation can be easily accelerated using GPUs and is useful even on deeper networks.

### C. Gradient Penalty

Gradient penalty (GP) [20] achieves the Lipschitz constraint required in Wasserstein GAN (WGAN) [21]. It replaces the

weight clipping of WGAN and effectively avoids the concentration of weights on the clipping threshold, so the network will not degenerate into a binary neural network. Besides, because it eliminates the setting of the clipping threshold, the network will not suffer from vanishing or exploding gradient because of the unreasonable threshold setting.

Although GP was originally used to improve WGAN, Wang *et al.* find that E-GAN and GP are orthogonal [3]. GP can be used to regularize the discriminator in E-GAN to support updating the generators.

## III. PRELIMINARIES

### A. Notation

We refer to the symbols used in [3], [22]. Most GANs can be formulated as:

$$L_D = \mathbb{E}_{x \sim p_{data}} [f_1(C(x))] + \mathbb{E}_{z \sim p_z} [f_2(C(h(T(z))))] \quad (1)$$

$$L_G = \mathbb{E}_{x \sim p_{data}} [g_1(C(x))] + \mathbb{E}_{z \sim p_z} [g_2(C(h(T(z))))] \quad (2)$$

where  $f_1, f_2, g_1, g_2$  are scalar-to-scalar functions, and the GAN and its variants with different loss functions correspond to these functions differently.  $p_{data}$  is the distribution of real data,  $p_z$  is the distribution of sampling noise (usually a uniform or normal distribution).  $T(z)$  is the nontransformed output of the generative network  $G$  and  $h(\cdot)$  is  $\tanh(\cdot)$  in deep convolutional GAN (DCGAN) [23].  $G(z) = h(T(z))$ , where  $G(z)$  is the output of the generator and its distribution  $p_g$  is expected to be fitted into  $p_{data}$ .  $C(x)$  is the nontransformed discriminator output. In most GANs,  $C(x)$  can be interpreted as how realistic the input data are [22]. In the original GAN,  $D(x) = \text{sigmoid}(C(x))$ , where  $D(x)$  is the output of the discriminative network  $D$ .

### B. Fitness Function

An evaluation criterion to measure the quality of individuals is needed in the evolutionary algorithm. Existing methods utilize various fitness functions, such as Inverted Generational Distance (IGD) [12], GAN objective [7], [9], Fréchet Inception Distance (FID) [7], [9], Koncept512 [11],  $F^{E-GAN}$  and its variants [3]–[6], and a mixture of them.

Fitness function  $F^{E-GAN}$  [3] consists of quality fitness  $F_q^{E-GAN}$  and diversity fitness  $F_d^{E-GAN}$ :

$$F^{E-GAN} = F_q^{E-GAN} + \gamma F_d^{E-GAN} \quad (3)$$

where  $\gamma > 0$  balances two measurements.

$$F_q^{E-GAN} = \mathbb{E}_{z \sim p_z} [D(G(z))] \quad (4)$$

The output of the discriminator  $D$  w.r.t. the generated samples  $G(z)$  are used as the quality fitness.

$$F_d^{E-GAN} = -\log \|\nabla_D - \mathbb{E}_{x \sim p_{data}} [\log D(x)] - \mathbb{E}_{z \sim p_z} [\log(1 - D(G(z)))]\| \quad (5)$$

The diversity fitness is the minus log-gradient-norm of the loss function of  $D$ . The logarithm is used to shrink the fluctuation of the gradient norm, which differs from the output of the discriminator  $D$  by an order of magnitude, and the amplitude

is so large that a simple balance coefficient cannot balance the two.

E-GAN argues that the more discrete the generated samples are, the less likely the discriminator is to change the parameters substantially.  $F_d^{E-GAN}$  embodies this principle. But our experiments show that  $F_d^{E-GAN}$  not only cannot achieve the design purpose, but also brings obvious side effects.

#### IV. METHOD

This section describes the details of our proposed IE-GAN, and introduces our research on crossover and evaluation. And a runnable algorithmic implementation of the framework is completed.

##### A. IE-GAN Framework

The framework IE-GAN designed in this paper evolves a population of generators  $G$  in a given dynamic environment (discriminator  $D$ ) and a static environment (diversity fitness function). Each individual in the population represents a possible solution in the parameter space [3]. IE-GAN framework is shown in Fig. 1.

In each evolutionary step, individuals  $\{G_{\theta_1}, \dots, G_{\theta_\mu}\}$  in the population  $G_\theta$  act as parents to generate offspring  $\{G_{\theta_{1,1}}, G_{\theta_{1,2}}, \dots, G_{\theta_{\mu,m}}\}$  by mutation operators. After evaluating them using fitness function  $F(\cdot)$ , the environmental fitness of mutation individuals is obtained. Then crossover parents are selected according to these fitness scores, and crossover individuals  $\{G_{\theta_{\mu+1,1}}, G_{\theta_{\mu+1,2}}, \dots, G_{\theta_{\mu+1,c}}\}$  are got by crossover operator. Next, evaluating the fitness of crossover individuals. Finally, the offspring with high fitness scores are selected as parents of the next generation.

After evolutionary step, the discriminator  $D$  is updated. Thus the dynamic environment also changes with the evolution of population, and is able to provide continuous evolutionary pressure in conjunction with static environment. The objective function of  $D$  is the same as that of the original GAN [1].

IE-GAN framework implemented in this paper adopts the same three mutation operators as E-GAN: minimax (GAN, [1]), heuristic (NS-GAN, [2]), and Least-squares (LSGAN, [24]). The complete algorithm is similar to Algorithm 2 in [14]. The required hyperparameters are: mutation batch size  $m$ , the updating steps of discriminator per iteration  $n_D$ , the number of parents  $\mu$ , the number of mutations  $n_m$ , the number of crossovers  $n_c$ , and Adam hyperparameters  $\alpha$ ,  $\beta_1$ ,  $\beta_2$ .

Compared to the two-player game of traditional GANs, E-GAN allows to select different dominant adversarial target in different training periods. Furthermore, CE-GAN [14] can integrate the advantages of multiple loss functions in each training period to generate advantageous individuals. Moreover, IE-GAN improves the crossover operator of CE-GAN and is able to guide evolution with a more accurate evaluation function, thereby obtaining a more competitive solution.

It is worth mentioning that the discriminator  $D$  is deeply involved in the whole process of the framework. It provides gradient information for mutation operators and it is an important measurement for evaluating samples and offspring. So the framework can benefit a lot from the improvement of  $D$ .

##### B. Mutation

IE-GAN framework does not care about the details of the genes encoded. Therefore, it has no hard and fast rules for the mutation operators, as long as the mutation operators can proliferate the parents into several different mutation individuals.

Benefiting from this, the IE-GAN framework can be easily applied to existing evolutionary GAN with generators as individuals, which do not introduce additional constraints.

##### C. Evaluation

FID is a common generation task metric in literature, which takes into account sample quality and diversity. It can also be used as fitness function to guide evolution in an evolutionary strategy. However, the higher time complexity makes it suitable only for methods with less evolutionary generations, otherwise the excessive time cost will make the method useless.

$F_d^{E-GAN}$  calculates the environmental fitness score of an individual by evaluating the  $l$  samples it generates. It splits the assessment metric into two aspects: quality fitness score and diversity fitness score. However, equation (5) cannot fully express the diversity fitness score. In fact,  $F_d^{E-GAN}$  is not only affected by diversity, but also by quality. As an example, if the generated sample distribution of an evaluation object hardly overlaps with the true sample distribution,  $D$  can discriminate the samples nearly 100%. When the  $D$  network hardly changes the parameters, the evaluation object will become unduly competitive. To put it simply, low quality samples will get high diversity fitness scores. This is the problem:  $F_d^{E-GAN}$  not only fails to reflect diversity, but also hinders the quality evaluation of  $F_q^{E-GAN}$ , which makes training vulnerable to vanishing gradient when the balance coefficient is not appropriate. Furthermore, the nonlinear scaling of  $F_d^{E-GAN}$  amplifies its negative effects, and even the most careful adjustment of the balance coefficients can easily make the evaluation results dominated by a single submetric.

In addition,  $F_d^{E-GAN}$  requires additional computation for the gradient information of discriminator, which increases the time cost significantly.

To solve these problems in E-GAN, we propose a new diversity fitness function, which estimates diversity in terms of mean absolute error (MAE) between samples. The generative diversity of individuals is measured by sample dissimilarity. Formally, our diversity fitness function is defined as follows:

$$F_d^{IE-GAN} = \frac{1}{n_e} \sum_i^{n_e} \mathbb{E}_{z_1, z_i \sim p_z} [\|G(z_1) - G(z_i)\|_1] \quad (6)$$

where the  $n_e$  refers to the number of times each sample is compared with other samples. It is the mean w.r.t. the MAE of each sample. The MAE of a single sample can also be considered as the evaluation of the sample itself, which helps the subsequent crossover operator to make full use of the evaluated samples. As shown in Fig. 2, our fitness function can objectively reflect the sample diversity.

Besides, our quality fitness function is also different from (4). We replace  $D(x)$  in  $F_q^{E-GAN}$  with the nontransformed

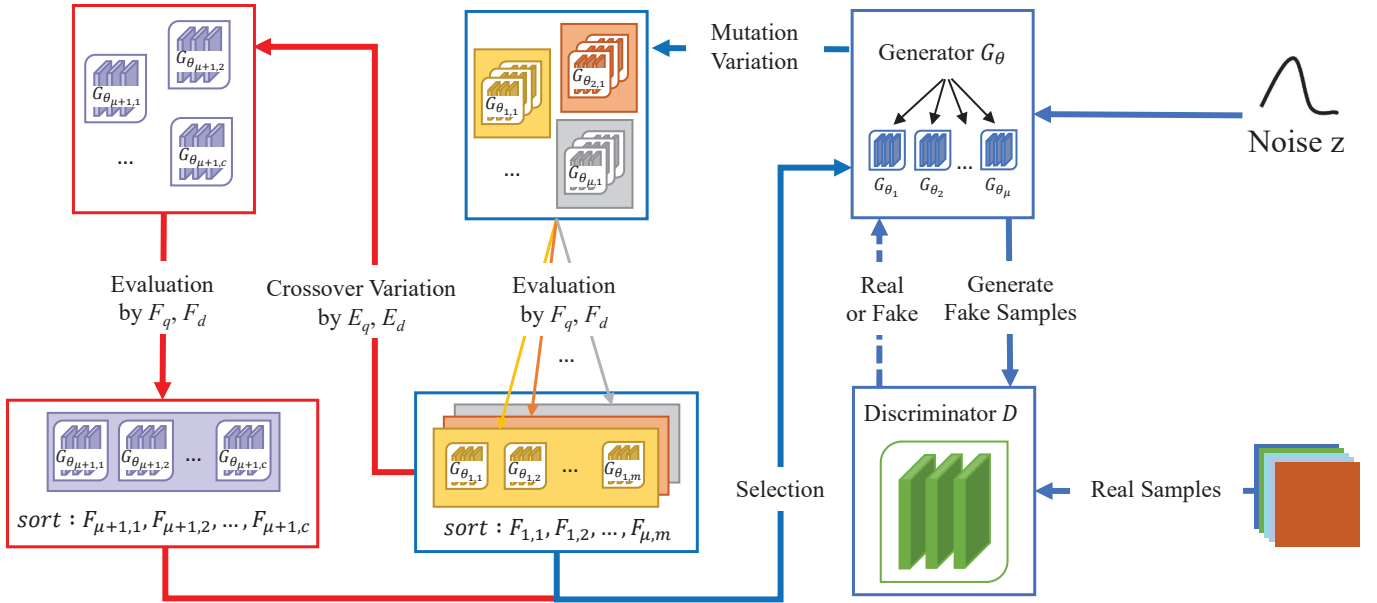


Fig. 1. The proposed IE-GAN framework. It adds crossover variation to take advantage of the experience of mutation individuals and enables a more efficient and accurate fitness evaluation function. The flow added in the evolutionary step is marked in red.

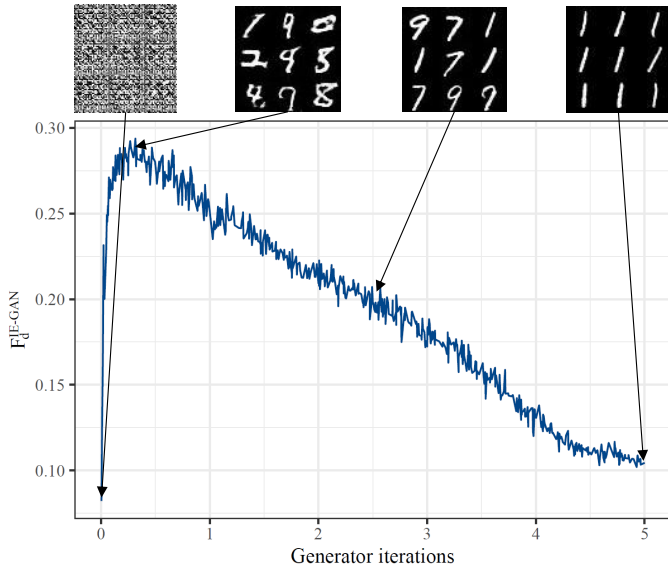


Fig. 2.  $F_d^{IE-GAN}$  curves and samples at different training stages. This figure only shows the correspondence between  $F_d^{IE-GAN}$  and sample diversity, and does not represent real experimental results.

discriminator output, i.e.,  $C(x)$ . The sigmoid layer does not change the sorting, but it does affect the output values. This may lead to changes in sorting when combined with diversity fitness. Compared to  $D(x)$ , we believe that  $C(x)$  is more representative of the quality of the input data. The formal definition of our quality fitness function is as follows:

$$F_q^{IE-GAN} = \mathbb{E}_{z \sim p_z} [C(G(z))] \quad (7)$$

Its essence is the evaluation of the sample quality by the discriminator. It can measure a single sample without addi-

tional operations, therefore it can be used to filter samples in crossover operator.

Combining the above two fitness functions, the fitness function of the IE-GAN framework can be obtained:

$$F^{IE-GAN} = F_q^{IE-GAN} + \gamma_1 F_d^{IE-GAN} \quad (8)$$

where  $\gamma_1 > 0$  balances the two metrics. A higher  $F^{IE-GAN}$  indicates that the evaluated object has better generative performance.

#### D. Crossover

In this subsection, we present the  $E$ -filtered knowledge distillation crossover w.r.t. the  $Q$ -filtered behaviour distillation crossover [18]. Due to the difference between GAN and RL, our crossover operator differs from it in some aspects including sample filtering and basis network selection. Fig. 3 illustrates the flow of a crossover variation.

The crossover operation of a pair of parent networks is as follows:

- The model with a higher fitness score among the parents is used as the basis of the offspring model, and the results generated by the parents with the same inputs are used as experiences for the offspring to imitate and learn.
- Transferring the knowledge of parents to offspring by means of knowledge distillation.

Note that the parents mentioned in the crossover refer to the mutation individuals generated by the mutation operators rather than the original parents of each generation.

The outputs of parents for the same inputs are likely to be completely different. So a natural question is that how should the offspring imitate both networks at the same time? The solution is that the child chooses the better output to imitate for each input. The definition of good or bad sample  $x$  is left

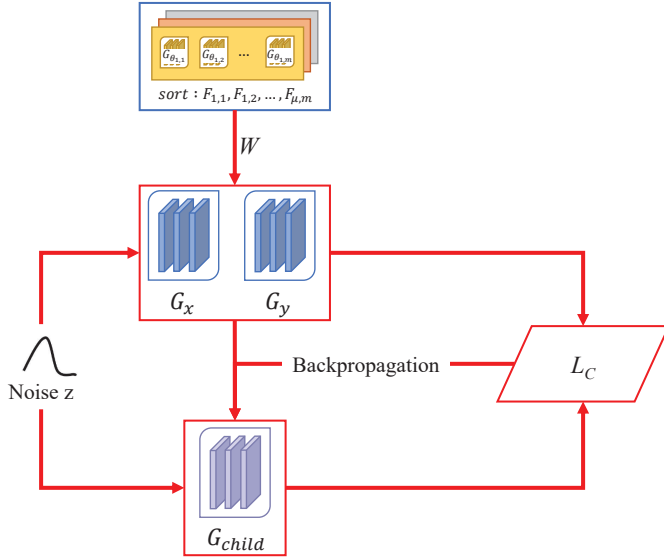


Fig. 3. The birth of a crossover offspring. Crossover parent pairs are selected from the mutation offspring according to the function  $W$ . The basic network of the crossover offspring is derived from the parents. For three networks with the same noise input, the offspring imitates learning by backpropagation of the loss function  $L_C$ .

to  $E(x)$ . The higher the  $E(x)$ , the more worthy of study.  $E(x)$  is defined as follows:

$$E = E_q + \gamma_2 E_d \quad (9)$$

This evaluation also considers both quality and diversity of samples.

$$E_q = C(x) \quad (10)$$

$$E_d = \frac{1}{n_e} \sum_i^{n_e} \mathbb{E}[\|x - x_i\|_1] \quad (11)$$

where  $x_i$  is a sample from the same batch as  $x$ .

The formal representation of the  $E$ -filtered knowledge distillation loss used to train the offspring is as follows:

$$L_C = \mathbb{E}_{E(G_x(z_i)) > E(G_y(z_i)) | z_i \sim p_z} [\|T_{child}(z_i) - T_x(z_i)\|^2] \\ + \mathbb{E}_{E(G_y(z_j)) > E(G_x(z_j)) | z_j \sim p_z} [\|T_{child}(z_j) - T_y(z_j)\|^2] \quad (12)$$

where  $G_x$  and  $G_y$  represent the generative strategies of parents.  $T_x(\cdot)$  and  $T_y(\cdot)$  are the inactive outputs of their corresponding generators, and  $T_{child}(\cdot)$  represents an inactive output of child. We believe that fitting with soft targets help the offspring inherit more information.

The offspring network learns the knowledge of parents by minimizing the function  $L_C$  during training. The whole procedure of the crossover operator is similar to Algorithm 1 in [14]. It needs the hyperparameter crossover batch size marked  $n$ .

There is still a problem: how to select parents from the multiple networks for crossover? We use the greedy strategy score function  $W$  defined in [18]:

$$W = F(G_x) + F(G_y) \quad (13)$$

This strategy usually results in the selection of better individuals, which ensures the excellence of the resulting offspring, and increases the stability of the population [18].

Since crossover parents and the initial network of crossover offspring need to be selected based on individual evaluation, it is necessary to evaluate mutation individuals before crossover. Given that both the assessment of individuals and samples are considered in terms of quality and diversity, the samples generated and the fitness scores obtained in the evaluation substage can be reused in the crossover substage.

This operator can act on the phenotype space [17] or the intermediate feature extraction [16]. Knowledge distillation does not care about the topological differences between teacher network and student network, but if learning from feature extraction, it is a challenge to select matches from the constantly changing network architecture for an evolutionary strategy that encodes topology as genes. In view of this, we choose to perform imitation learning from the end of network so that it can be applied to a more general framework.

The crossover operator proposed in this paper is somewhat different from the biological sense of crossover variation. In biology, the phenotypic traits of offspring are determined by gene expression, and the dominance of inherited traits is reflected by the dominance of genes (usually the traits represented by dominant genes are better). In short, gene crossover determines trait inheritance. The basis for the realization of our crossover operator is learning of the expression of parental superior traits in the phenotype space and inscribing the knowledge in the network weights. The superior traits are judged by the offspring themselves. The entire process does not require the participation of genes, and because of this gene-independence, the  $E$ -filtered knowledge distillation crossover operator does not care about the genes encoded by the individuals of the population.

### E. Selection

There are two questions on the selection of the next generation parents: whether the mutation individuals are still candidates? And whether the current parents are candidates?

For the former question, we have experimentally demonstrated that only using crossover offspring will not bring significant gains, and doing so does not reduce the computational complexity. Therefore, mutation offspring should not be excluded from selection.

As for the latter issue, existing studies use updated discriminators to re-evaluate current parents and treat them as parent candidates for the next generation [4], [6]. Experiments on our framework show that this strategy enhances training stability. But it will slow down convergence, drag down the final result and increase computational effort. So we do not consider transferring the current parents to the next generation.

## V. EXPERIMENTS

To verify the effectiveness of the IE-GAN framework, we experiment with its algorithmic implementation on several generative tasks and present the results in this section. The

experiments show that IE-GAN can achieve competitive performance with high efficiency. In addition, we analyze some details of the method.

### A. Experimental Configuration

We conduct experiments on two synthetic datasets and two real-world image datasets: CIFAR-10 [25] and CelebA [26]. The two synthetic datasets are a 2D mixture of 8 Gaussians arranged in a circle and a 2D mixture of 25 Gaussians arranged in a grid. Because the distribution of generated data and target data can be visualized, such toy datasets are often used to demonstrate the mode collapse of the method. CIFAR-10 is a dataset for identifying universal objects, containing 10 categories of RGB color images about objects in the real world. The images in it are not only noisy, but the proportions and features of the objects are also different, which brings great difficulties to recognition. The size of the images is  $32 \times 32$ . CelebA is a large-scale face attribute dataset with a large number of celebrity images. The images in this dataset cover pose variations and background clutter.

For comparison purposes, the networks of generators and discriminator on CIFAR-10 are the same as E-GAN [3], which are fine-tuned DCGAN networks [23]. As for CelebA, we adopt the official PyTorch implementation of the DCGAN network architecture which is available at <https://github.com/pytorch/examples/tree/master/dcgan>. To cope with the complex dataset CelebA, we apply more channels in the convolutional layers and transposed convolutional layers. In addition, we choose multilayer perceptron (MLP) as the model architecture for the toy experiments. The target distribution of synthetic data and the corresponding network architectures in the experiments are taken from the third-party PyTorch implementation code of WGAN-GP at <https://github.com/caogang/wgan-gp>. The model architecture applied in this paper is shown in detail in Table. I.

The values of hyperparameters shared with E-GAN are the same, specifically,  $\alpha = 2e - 4$ ,  $\beta_1 = 0.5$ ,  $\beta_2 = 0.999$ ,  $n_D = 3$ ,  $n_m = 3$ ,  $m = 32$ ,  $l = 256$ . But the balance coefficients of fitness quality and diversity (i.e.,  $\gamma_1$ ) is an exception. This is due to we redefine the quality and diversity fitness function. We select  $\gamma_1 = 1$  for the synthetic datasets and  $\gamma_1 = 0.05$  for the real-world datasets via grid search. Normally, we take the population size  $\mu = 1$ . For IE-GAN specific hyperparameters, we choose  $\gamma_2 = 0.001$ ,  $n_e = 5$ , and  $n_c = 1$  for all experiments. Apart from that, we set the crossover batch size  $n$  to 256, which equals  $l$ . In this paper, we will conduct experiments with these values if not otherwise stated.

We use FID [13] to quantitatively evaluate the generative performance. FID is frequently used as a metric in researches regarding GANs, and it is considered superior to other metrics [27]. The lower the FID, the better the quality of the generated images. We randomly generate 50k images to calculate FID for the Tensorflow code version. Without special instructions, the experiments in this paper will be trained for 100k generations.

The experiments are conducted on a single NVIDIA TITAN Xp GPU with 12GB memory and Intel Xeon E5-2620 v2 CPU.

The code we implemented in PyTorch is publicly available at <https://github.com/AlephZr/IE-GAN>.

### B. Mode Collapse

Learning the 2D Gaussian mixture distribution can visually demonstrate the mode collapse of the model. If the model suffers from mode collapse, the samples it generates will focus on a limited number of modes. And this can be directly observed and compared through Kernel Density Estimation (KDE) plots.

We compare the complete algorithm of IE-GAN with the baselines including GAN, NS-GAN, LSGAN, and E-GAN. For fairness, all methods utilize the same MLP network architecture. Because of the huge difference between synthetic and real-world datasets, the learning rate and the number of discriminator updates in each iteration are consistent with the source of the network architecture, namely  $\alpha = 1e-4$ ,  $n_D = 1$ .

Fig. 4 illustrates the modes captured by different methods. The center plot of each plot is the KDE plot, and the side plots reflect the probability distribution. To adequately represent the generated distribution, 10240 points are sampled for each plot. We can see that on both synthetic datasets, the baselines show more or less mode missing. This is especially true for E-GAN, which appears to be inapplicable to experimental networks. It performs the worst of all methods, and its evolutionary strategy exacerbates mode collapse. Whereas IE-GAN is able to cover all modes (although some modes are weakly covered), which indicates that our evolutionary strategy can effectively suppress mode collapse. This is corroborated by side plots, where the probability distribution of IE-GAN is the closest to the target data.

### C. Generative Performance and Time Cost

To illustrate the superiority of proposed IE-GAN over baselines, we conduct experiments on the CIFAR-10 dataset. The baselines used for comparison include GAN-Minimax, GAN-Heuristic, and GAN-Least-squares which respectively represent the method of using the corresponding single mutation operator. The experimental results obtained by comparing with these baselines are used to demonstrate that our approach benefits primarily from the framework rather than network architecture. In order to explore the role of each operator, their settings are identical to IE-GAN, including  $n_D$  and discriminator objective functions. In addition, we compare with E-GAN [3] to demonstrate the effectiveness of the proposed evolutionary strategy. E-GAN likewise maintains only 1 population when not specifically stated.

Fig. 5 plots FID for training process of different methods under the same network architecture. The objects marked with “-GP” here and after indicate that GP term is used. We use experimental setup from the literature [3] with codes provided by authors at <https://github.com/WANG-Chaoyue/EvolutionaryGAN-pytorch> to obtain the results of E-GAN. If not indicated, E-GAN maintains the population  $\mu = 1$ . As can be seen from this figure:

- The GP term is orthogonal to IE-GAN, and IE-GAN behaves more significantly than E-GAN in terms of the improvement of the GP term on the generative performance.

TABLE I  
Architectures of the Generative and Discriminative Networks.

Generative network	Discriminative network
<b>E-GAN</b> <b>Input:</b> Noise $z \sim p_z$ , 100 [layer 1] Transposed Convolution (4, 4, 512), stride=1; <i>ReLU</i> ; [layer 2] Transposed Convolution (4, 4, 256), stride=2; <i>ReLU</i> ; [layer 3] Transposed Convolution (4, 4, 128), stride=2; <i>ReLU</i> ; [layer 4] Transposed Convolution (4, 4, 3), stride=2; <i>Tanh</i> ; <b>Output:</b> Generated Image, $(32 \times 32 \times 3)$	<b>Input:</b> Image, $(32 \times 32 \times 3)$ [layer 1] Convolution (4, 4, 128), stride=2; <i>LeakyReLU</i> ; [layer 2] Convolution (4, 4, 256), stride=2; Batchnorm; <i>LeakyReLU</i> ; [layer 3] Convolution (4, 4, 512), stride=2; Batchnorm; <i>LeakyReLU</i> ; [layer 4] Fully connected (1); <i>Sigmoid</i> ; <b>Output:</b> Real or Fake (Probability)
<b>DCGAN</b> <b>Input:</b> Noise $z \sim p_z$ , 100 [layer 1] Transposed Convolution (4, 4, 1024), stride=1; Batchnorm; <i>ReLU</i> ; [layer 2] Transposed Convolution (4, 4, 512), stride=2; Batchnorm; <i>ReLU</i> ; [layer 3] Transposed Convolution (4, 4, 256), stride=2; Batchnorm; <i>ReLU</i> ; [layer 4] Transposed Convolution (4, 4, 128), stride=2; Batchnorm; <i>ReLU</i> ; [layer 5] Transposed Convolution (4, 4, 3), stride=2; <i>Tanh</i> ; <b>Output:</b> Generated Image, $(64 \times 64 \times 3)$	<b>Input:</b> Image, $(64 \times 64 \times 3)$ [layer 1] Convolution (4, 4, 128), stride=2; <i>LeakyReLU</i> ; [layer 2] Convolution (4, 4, 256), stride=2; Batchnorm; <i>LeakyReLU</i> ; [layer 3] Convolution (4, 4, 512), stride=2; Batchnorm; <i>LeakyReLU</i> ; [layer 4] Convolution (4, 4, 1024), stride=2; Batchnorm; <i>LeakyReLU</i> ; [layer 5] Convolution (4, 4, 1), stride=1; <i>Sigmoid</i> ; <b>Output:</b> Real or Fake (Probability)
<b>MLP</b> <b>Input:</b> Noise $z \sim p_z$ , 2 [layer 1] Fully connected (512); <i>ReLU</i> ; [layer 2] Fully connected (512); <i>ReLU</i> ; [layer 3] Fully connected (512); <i>ReLU</i> ; [layer 4] Fully connected (2); <b>Output:</b> Generated Point, $(2 \times 1)$	<b>Input:</b> Point, $(2 \times 1)$ [layer 1] Fully connected (512); <i>ReLU</i> ; [layer 2] Fully connected (512); <i>ReLU</i> ; [layer 3] Fully connected (512); <i>ReLU</i> ; [layer 4] Fully connected (1); <i>Sigmoid</i> ; <b>Output:</b> Real or Fake (Probability)

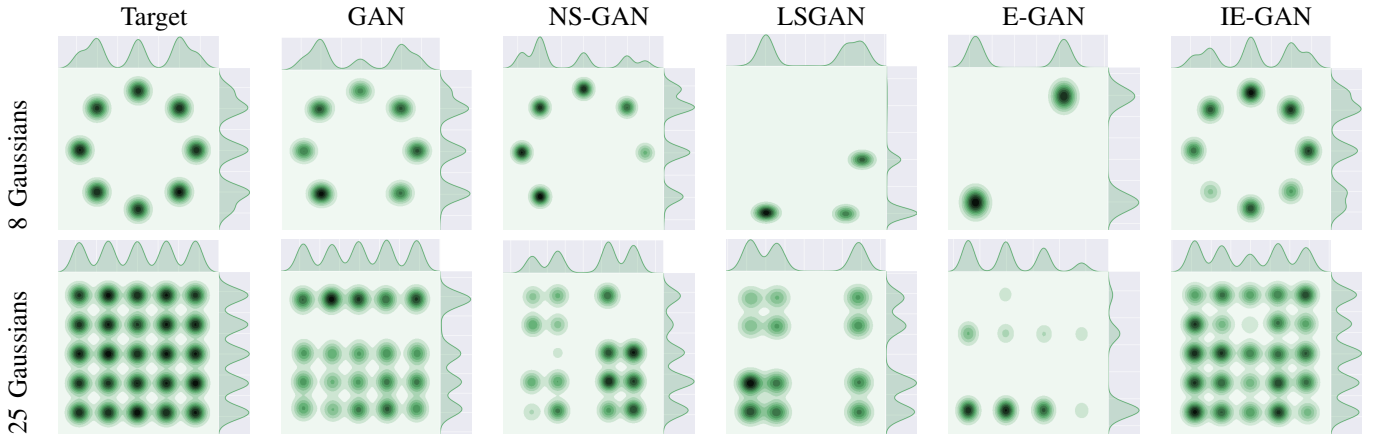


Fig. 4. KDE plots of the target data and the generated data of various GANs trained on the synthetic dataset. The first row is 8 Gaussian mixture distribution, which is trained for only 30k iterations because of the small number of modes. The second row is 25 Gaussian mixture distribution, trained for 100k iterations.

This is because the GP term acts on the discriminator, which is more deeply involved in IE-GAN. In addition to the normal gradient learning and participation in the evaluation as in E-GAN, the discriminator in IE-GAN also takes part in the assessment of the samples during the crossover process. Therefore, IE-GAN can benefit more from the discriminator enhancement.

- The GP term also accelerates the convergence of IE-GAN, whereas E-GAN has no such performance. This is the work of crossover operator. The discriminator is involved in crossover variation, so a better discriminator helps to obtain better crossover offspring, which in turn accelerates model convergence.
- The crossover operator itself also contributes to convergence. IE-GAN shows considerable convergence speed, and it is clearly distinguished from methods other than IE-GAN-GP until 25k iterations.
- IE-GAN does benefit from multiple operators, and IE-

GAN-GP has the best generative performance and the fastest convergence speed. Most of the time, the fold line representing it is at the bottom.

- The evolutionary strategy of E-GAN works the other way around. Under the same conditions, E-GAN-GP is worse than any of the single mutation operator methods. Its generative performance is only similar to that of IE-GAN without GP term.

For comparison and analysis, the FID of different methods including various populations of E-GAN are listed in Table. II, where the data marked with † are quoted from [3]. “Final FID” in the table denotes the FID after 100k iterations. The best value is bolded. We reproduced the multipopulation experiments of E-GAN, but perhaps because of the different experimental environments, the final results are different from those in [3]. The results of our experiment show that:

- The generative performance of E-GAN can be improved by increasing the population, but it is insignificant. As the

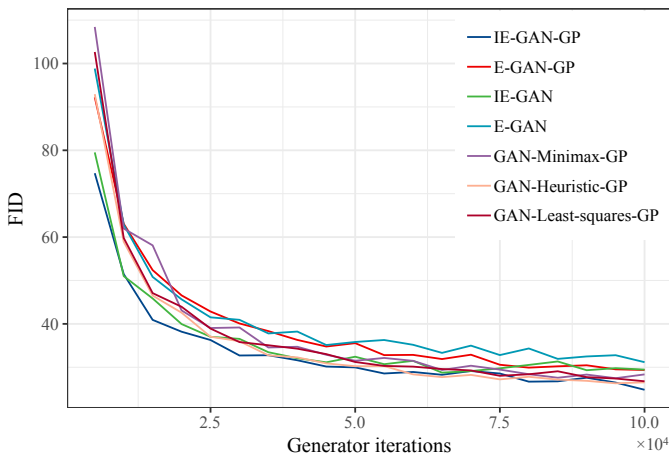


Fig. 5. FID of different methods on CIFAR-10 over generator iteration.

TABLE II  
FID of Different Methods and Various Populations.

Methods	Final FID
GAN-Minimax-GP	28.36
GAN-Heuristic-GP	26.53
GAN-Least-squares-GP	26.77
E-GAN ( $\mu = 1$ )†	36.2
E-GAN-GP ( $\mu = 1$ )†	33.2
E-GAN-GP ( $\mu = 2$ )†	31.6
E-GAN-GP ( $\mu = 4$ )†	29.8
E-GAN-GP ( $\mu = 8$ )†	27.3
E-GAN ( $\mu = 1$ )	31.18
E-GAN-GP ( $\mu = 1$ )	29.38
E-GAN-GP ( $\mu = 2$ )	28.84
E-GAN-GP ( $\mu = 4$ )	30.46
E-GAN-GP ( $\mu = 8$ )	28.45
(Ours) IE-GAN ( $\mu = 1$ )	29.47
(Ours) IE-GAN-GP ( $\mu = 1$ )	<b>24.82</b>

population size increases from 1 to 8, the FID decreases by just less than 1, and the number of maintained generative networks increases from 3 to 24, which increases the cost.

- This improvement of E-GAN is also unstable. When  $\mu = 4$ , the experimental results are rather worse than  $\mu = 1$ .
- E-GAN does not benefit from plural operators. The population brings such a small improvement that the performance of  $\mu = 8$  is likely to be close to the limit that E-GAN can achieve. Even so, E-GAN-GP is still inferior to GAN-Minimax-GP, which is the worst single mutation operator method. The results show that, due to the unreasonable evaluation function, E-GAN performs worse than any reference object.

Runtime is also an important criterion for evaluating method usability. Fig. 6 shows wall-clock time of training different methods 100k iterations on the CIFAR-10 dataset, and the length of bar reflects time cost of the corresponding method.

The GAN-Minimax, GAN-Heuristic, and GAN-Least-squares maintain only one generator network and no additional evaluation of the generators is required, so the time cost for training is less and similar. IE-GAN costs just over twice as

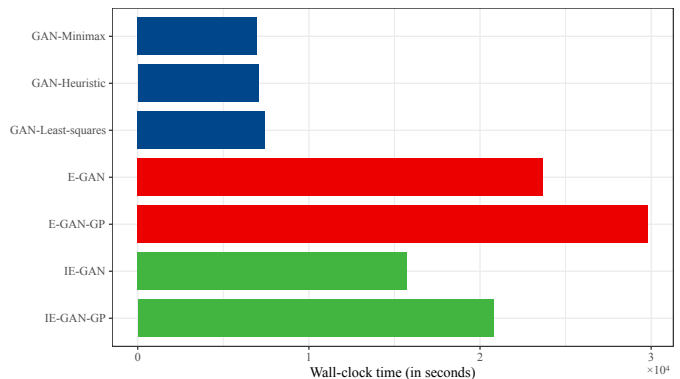


Fig. 6. Wall-clock time of different methods.

much time as them while maintaining four generative networks. Even with GP term added, the time cost is about three times that of them. The relative simplicity of  $F_d^{IE-GAN}$  and the reuse of individual evaluation results when assessing the sample contribute to this. E-GAN does not contain crossover operator and does not need to maintain crossover individuals. However, although there are fewer generative networks, it takes much more time than IE-GAN. This is mainly due to the extra calculation of the discriminator gradient information by  $F_d^{E-GAN}$ . With the increase in the number of parents  $\mu$ , the time required to calculate  $F_d^{E-GAN}$  becomes more and more nonnegligible.

#### D. Ablation Study

We compare IE-GAN with ablation variants of it. Fig. 7 shows examples in the synthetic datasets. Eliminating  $F_d^{IE-GAN}$  or crossover variation decreases performance and eliminating both together leads to more serious consequences. This means that both  $F_d^{IE-GAN}$  and crossover support generative diversity.

Similar conclusion can be obtained on the CIFAR-10 dataset. Fig. 8 shows that both items are critical to our method. In addition, the crossover operator exhibits its acceleration effect.

#### E. Hyperparameters Analysis

We use the same discriminator objective function as E-GAN.

There are two more hyperparameters that are closely related to the performance of IE-GAN, namely the balance coefficient of fitness function ( $\gamma_1$ ) and sample evaluation function ( $\gamma_2$ ). Since they are used to balance quality and diversity measurements, they guide the selection of generators and samples, which affects the performance of IE-GAN. Meanwhile, the targets of knowledge distillation of crossover operator, the number of parents imitated by crossover offspring, the size of crossover batch size  $n$ , and the times of sample comparisons  $n_e$  all affect the effectiveness of IE-GAN. In this section, we will analyze their effects one by one through experiments on CIFAR-10.



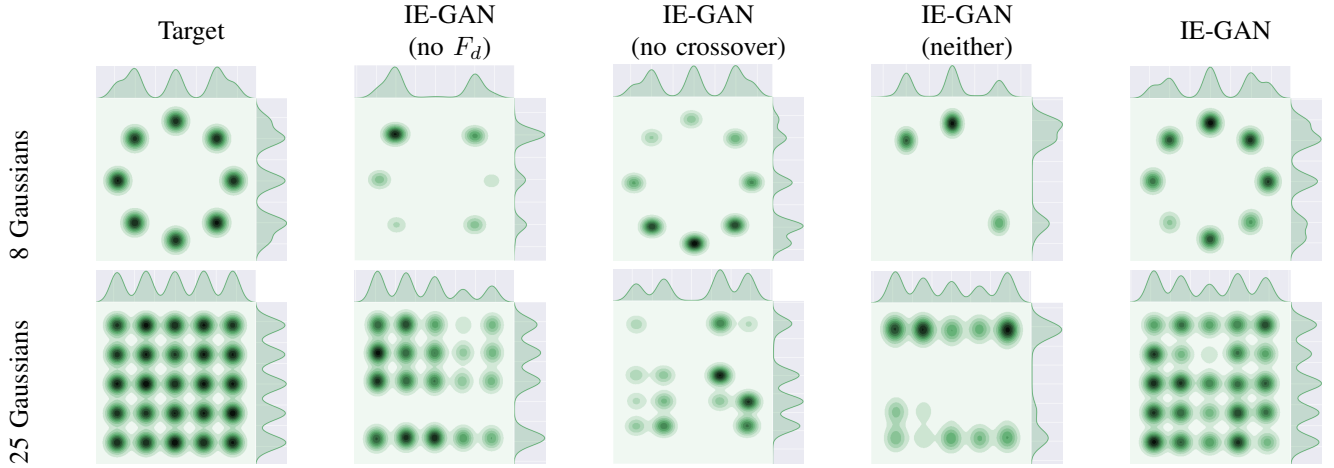


Fig. 7. KDE plots for ablation study. The first row is 8 Gaussian mixture distribution, trained for 30k iterations. The second row is 25 Gaussian mixture distribution, trained for 100k iterations. “no  $F_d$ ” indicates that IE-GAN does not use the diversity fitness function  $F_d^{IE-GAN}$ . “no crossover” indicates that IE-GAN does not apply crossover variation. “neither” indicates that IE-GAN has neither.

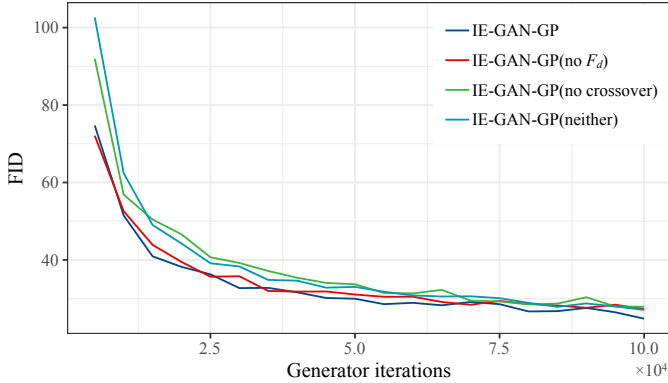


Fig. 8. FID for ablation study. “no  $F_d$ ” indicates that IE-GAN does not use the diversity fitness function  $F_d^{IE-GAN}$ . “no crossover” indicates that IE-GAN does not apply crossover variation. “neither” indicates that IE-GAN has neither.

1)  $\gamma_1$ : In order to guarantee confidence, we choose a larger population to ensure that there are enough individuals for each evaluation. In this way, the effect of balance coefficient  $\gamma_1$  can be amplified so that the performance of the generators is sufficiently differentiated. In this experiment, the population size is set to  $\mu = 4$ .

Given a large number of individuals, a discriminator with GP term is employed against it to achieve stable training. To eliminate the interference of the crossover operator and related hyperparameters, the crossover operator is not enabled in this experiment.

We perform a grid search to find the appropriate value for  $\gamma_1$ . Table. III lists the performance measurements of the trained generators, the balance coefficient  $\gamma_1 \in \{0, 0.001, 0.01, 0.05, 0.1, 0.5, 1\}$  are taken for the experiment. When  $\gamma_1 = 0$ ,  $F_d^{IE-GAN}$  is not enabled. “Best FID” in the table represents the best FID of the method during the training

TABLE III  
FID for Various Fitness Balance Coefficient.

Methods	Final FID	Best FID
IE-GAN-GP ( $\gamma_1 = 0$ , w/o crossover)	27.38	27.38
IE-GAN-GP ( $\gamma_1 = 0.001$ , w/o crossover)	28.11	27.59
IE-GAN-GP ( $\gamma_1 = 0.01$ , w/o crossover)	27.79	27.79
IE-GAN-GP ( $\gamma_1 = 0.05$ , w/o crossover)	<b>27.15</b>	<b>26.74</b>
IE-GAN-GP ( $\gamma_1 = 0.1$ , w/o crossover)	27.21	27.21
IE-GAN-GP ( $\gamma_1 = 0.5$ , w/o crossover)	27.86	27.56
IE-GAN-GP ( $\gamma_1 = 1$ , w/o crossover)	27.73	27.73

process. The best value for each item is bolded.

Whether it is final FID or best FID, these values generally decrease first and then increase as  $\gamma_1$  increases. The exception is  $\gamma_1 = 0$ , which has better score than any of the methods outside  $\gamma_1 \in \{0.05, 0.1\}$ . This suggests that an inappropriate additional term is more likely to be a source of interference. The results show that the performance is correlated with the  $\gamma_1$ , which leads to poorer consequences whether it is too large or too small. This phenomenon occurs in experiments with different population sizes. We select  $\gamma_1 = 0.05$  for real-world image datasets based on observations.

2)  $\gamma_2$  *Correlation*: Softer targets are preferred in knowledge distillation, which can minimize information loss. In principle, our crossover operator allows the offspring to learn from a set of networks rather than a limited set of 2 parents. This is a tempting idea, which means that the crossover offspring can absorb more experience from the trained network.

Also, the balance coefficient of the sample evaluation function  $\gamma_2$  directly controls the learning objects of offspring, which is similar to  $\gamma_1$ . However,  $\gamma_2$  should not be roughly equal to  $\gamma_1$ , because they serve different purposes.

Since all three hyperparameters ( $\gamma_2$ , knowledge distillation targets, and crossover parents number) are related to the crossover operator and are tightly correlated, they are considered together here. We perform a grid search for  $\gamma_2 \in \{0, 0.0001, 0.001, 0.01, 0.1, 1\}$  in a total of four contexts

combined with different knowledge distillation targets and crossover parents number. We set the size of population  $\mu = 1$  and the crossover number  $n_c = 1$  in this experiment. The performance measurements are reported in Table. IV. The best of each context is bolded and the best of all contexts is additionally underlined.

Within each context, equation (11) is counterproductive when  $\gamma_2$  is inappropriate, and  $E_d$  gradually takes on a positive effect as  $\gamma_2$  tends to 0.001 in general. Whereas this is not true in the context of hard targets with all mutation offspring as crossover parents, its FID is abnormal at  $\gamma_2 = 0.001$ . We believe that the outlier is due to the randomness of the experiment. In summary, we set  $\gamma_2$  to 0.001. Experiments show that this value is applicable to both real-world image datasets and synthetic datasets.

The comparison between contexts can support the choice of the other two hyperparameters. The crossover operator with soft targets is more promising than that with hard targets as expected. However, more crossover parents do not bring greater advantages. With both soft and hard targets, the results of the 2-parent methods are mostly better than the methods with more parents, both in terms of final FID and best FID. Therefore, our crossover operator employs soft targets in knowledge distillation and learns experience from only one pair of parents.

We presume that the reason for the negative impact of more crossover parents is that  $E$  does not fit reality well enough. The fixed balance coefficient  $\gamma_2$  constrains the efficiency of  $E$ . Intuitively, as Fig. 2 illustrates, quality evaluation is more important in the early stage of training, when normal training can boost diversity at a high rate; whereas diversity evaluation is more important in the later stage of training, when quality is difficult to improve and diversity loss should be avoided as much as possible. And the effectiveness of methods can be ensured by limiting the influence of this underfitting function on the training process, so that a pair of crossover parents is more favorable for our work.

3) *Other*: To verify this presume, we enlarge population, increase the number of crossover offspring, and conduct experiments. Based on the reality that  $\gamma_1$  suffers from the same problem as  $\gamma_2$ , the number of evaluated individuals should be negatively correlated with the generative performance.

As shown in Fig. 9, larger population brings almost only negative effects: slow convergence, unstable training, and poor FID. This confirms our conjecture that in the face of a larger population,  $F^{IE-GAN}$  seems to be a little weak. Therefore, we recommend that the population maintain only one size.

Whereas more crossover offspring perform relatively well, IE-GAN with  $n_c = 3$  reflects advantage in having a similar number of generative networks as IE-GAN with  $\mu = 2$ . It accelerates the convergence and its best FID is comparable to that of a single crossover offspring. This is perhaps due to the excellent crossover operator itself, which improves the fault tolerance of evaluation. But probably because of the fast convergence, it appears to be a bit over-fitting in the late stage. And it does not observably improve FID. Considering the increase in computing overhead due to more generative networks, we choose  $n_c = 1$ .

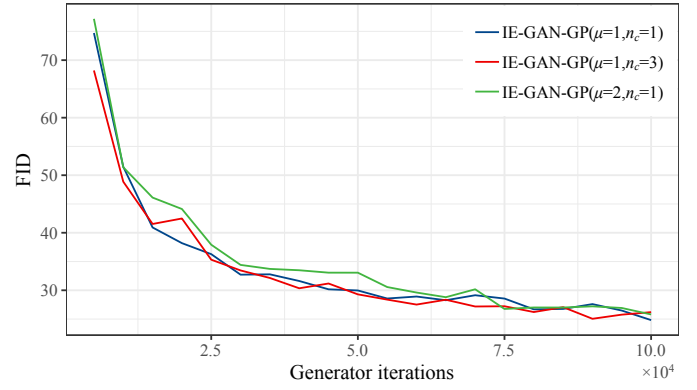


Fig. 9. FID of different IE-GANs with various crossover size  $n_c \in \{1, 3\}$  and population size  $\mu \in \{1, 2\}$ .

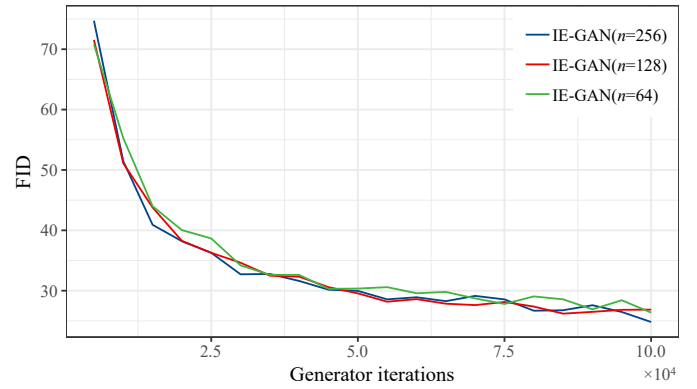


Fig. 10. FID of different IE-GANs with various crossover batch size  $n \in \{256, 128, 64\}$ .

The crossover operator transfers the experience of parental networks by means of knowledge distillation, and crossover batch size  $n$  determines the magnitude of experience that offspring can contact. Logically, the larger the  $n$  is, the deeper the offspring understands the parental strategy and the better it inherits the superior traits. We conduct experiments on this and record the results in Fig. 10.

As expected, the experiments show that the competitiveness of method is positively correlated with  $n$  within a certain range. Along with the increase of  $n$ , IE-GAN has improved in convergence speed, stability, and generative performance. The crossover batch size  $n$  is set to 256 in this paper, which is consistent with the number of samples when calculating fitness. As mentioned earlier, it is an established matter to evaluate the fitness of mutation offspring before crossover variation. Fully reusing the results of evaluation, including generated samples and single-sample evaluation, can accommodate both performance and time cost.

We also conduct experiments about  $n_e$ , and the results are listed in Table. V.  $n_e$  represents how many samples each sample should be compared with when scoring diversity. It is not better to have a large number, if it is too large it can easily lead to duplicate comparisons and more computation. But if  $n_e$  is too small, the samples cannot be effectively distinguished and  $F_d^{IE-GAN}$  does not work. We think  $n_e = 5$  is appropriate.

TABLE IV  
FID for Various Knowledge Distillation Targets, Crossover Parents Size, and Sample Evaluation Balance Coefficient.

	Soft targets			Hard targets		
	Methods	Final FID	Best FID	Methods	Final FID	Best FID
Parents 2	IE-GAN-GP ( $\gamma_2 = 0$ )	25.79	25.74	IE-GAN-GP ( $\gamma_2 = 0$ )	25.65	25.65
	IE-GAN-GP ( $\gamma_2 = 0.0001$ )	26.11	26.11	IE-GAN-GP ( $\gamma_2 = 0.0001$ )	26.17	26.17
	IE-GAN-GP ( $\gamma_2 = 0.001$ )	<b>24.82</b>	<b>24.82</b>	IE-GAN-GP ( $\gamma_2 = 0.001$ )	<b>25.63</b>	<b>25.63</b>
	IE-GAN-GP ( $\gamma_2 = 0.01$ )	27.49	25.70	IE-GAN-GP ( $\gamma_2 = 0.01$ )	26.52	26.52
	IE-GAN-GP ( $\gamma_2 = 0.1$ )	26.27	25.82	IE-GAN-GP ( $\gamma_2 = 0.1$ )	25.84	25.84
	IE-GAN-GP ( $\gamma_2 = 1$ )	26.02	26.02	IE-GAN-GP ( $\gamma_2 = 1$ )	27.08	26.34
Parents all	IE-GAN-GP ( $\gamma_2 = 0$ )	26.71	26.23	IE-GAN-GP ( $\gamma_2 = 0$ )	26.63	26.37
	IE-GAN-GP ( $\gamma_2 = 0.0001$ )	26.13	26.13	IE-GAN-GP ( $\gamma_2 = 0.0001$ )	<b>26.19</b>	26.19
	IE-GAN-GP ( $\gamma_2 = 0.001$ )	<b>25.81</b>	<b>25.81</b>	IE-GAN-GP ( $\gamma_2 = 0.001$ )	26.64	26.64
	IE-GAN-GP ( $\gamma_2 = 0.01$ )	26.36	26.36	IE-GAN-GP ( $\gamma_2 = 0.01$ )	26.21	<b>25.94</b>
	IE-GAN-GP ( $\gamma_2 = 0.1$ )	26.70	26.70	IE-GAN-GP ( $\gamma_2 = 0.1$ )	27.82	26.45
	IE-GAN-GP ( $\gamma_2 = 1$ )	26.31	26.07	IE-GAN-GP ( $\gamma_2 = 1$ )	26.79	26.79

TABLE V  
FID for Various Number of Sample Comparisons.

Methods	Final FID	Best FID
IE-GAN-GP ( $n_e = 1$ )	26.66	26.66
IE-GAN-GP ( $n_e = 3$ )	26.07	25.54
IE-GAN-GP ( $n_e = 5$ )	<b>24.82</b>	<b>24.82</b>
IE-GAN-GP ( $n_e = 30$ )	26.70	26.20
IE-GAN-GP ( $n_e = 256$ )	27.15	26.58

TABLE VI  
FID for Diversity Fitness Function (w/o Crossover).

Methods	Final FID	Best FID
IE-GAN-GP ( $\mu = 1$ , quality fitness)	<b>27.06</b>	27.06
IE-GAN-GP ( $\mu = 1$ )	27.90	27.90
IE-GAN-GP ( $\mu = 4$ )	27.15	<b>26.74</b>
E-GAN-GP ( $\mu = 1$ )	29.38	29.38
E-GAN-GP ( $\mu = 8$ )	28.45	—

### F. Diversity Fitness Function Analysis

A notable feature of E-GAN is that the heuristic objective and the least-squares objective are frequently selected in the early stage (first 20k iterations) [3]. And heuristic objective is selected more frequently than least-squares.

We reproduce the experiments in the literature of E-GAN on CIFAR-10 dataset, but we are unable to obtain similar results. As shown in Fig. 11(a), using the code provided by the authors at the same balance coefficient as E-GAN ( $\gamma = 0.001$ ), least-squares objective has the absolute advantage. We carefully adjusted the  $\gamma$ , but still cannot reproduce the results in the literature of E-GAN.

It can be seen from Fig. 11(a) that the selection tendency is related to the value of  $\gamma$ : as the  $\gamma$  increases, the proportion of least-squares objective decreases and the proportion of heuristic and minimax objective increases subsequently. However, whether  $\gamma$  is small or large, least-squares objective or minimax objective rather than heuristic objective is dominant. Moreover, this process is accompanied by the risk of vanishing gradient, such as  $\gamma \in \{0.003, 0.007, 0.1, 1.0\}$  in Fig. 11(a). Due to the weakness of minimax objective, the offspring generated in the early stage can be easily distinguished by the discriminator, while  $F_d^{E-GAN}$  gives an unreasonably high fitness score, which leads to the occurrence of vanishing gradient.

The method with frequent selection of least-squares objective can be trained successfully and the frequency of the other two being selected in the subsequent training is improved, as shown in Fig. 11(b), which shows the selected rate after full training. And the method of choosing minimax objective all the time will lead to vanishing gradient.

In view of the sensitivity of  $F^{E-GAN}$  to  $\gamma$ , we believe that the method is not usable even if we are lucky to find values to achieve the purpose, so we abandoned this attempt.

The effect of the diversity fitness function is demonstrated by Table. VI. ‘‘Quality fitness’’ indicates that only  $F_q$  is used for the evaluation. IE-GANs discard the crossover operator. At this point, IE-GAN with quality fitness is equivalent to E-GAN using only  $F_q^{E-GAN}$ .

Experimental results show that  $F_d^{E-GAN}$  limits performance and even reduces performance. By simply removing this time-costly component, the generative performance of IE-GAN-GP with quality fitness (which can be regarded as E-GAN-GP with quality fitness) has significant improvement compared to E-GAN-GP. Whereas  $F_d^{IE-GAN}$  does not have such an obvious side effect. The degradation of IE-GAN is much less than E-GAN.

The gain of E-GAN due to multipopulation compensate for the negative effect of  $F_d^{E-GAN}$ . Moreover, even maintaining a population of 8 individuals, E-GAN-GP is worse than the method that simply uses quality fitness function. Relatively, IE-GAN using  $F_q^{IE-GAN}$  can outperform IE-GAN using  $F_q^{E-GAN}$  because of the increase in population.

### G. Crossover Operator Analysis

In the implementation of PDERL (<https://github.com/crisbodnar/pderl>),  $Q$ -filtered behaviour distillation crossover chooses a less capable network as the initial child, whereas we choose the better one, which arises from the difference between GAN and RL. The networks of GAN tend to be deeper, the generated samples are more time-sensitive, and the sample batch size is smaller to improve efficiency.

To demonstrate it, we experimentally compare the two crossover operators, i.e., based on better parent and based on worse parent. The fitness of offspring is a good indicator to measure quality of crossover operator. Fig. 12 plots ten randomly selected parent pairs, each set of bars includes the

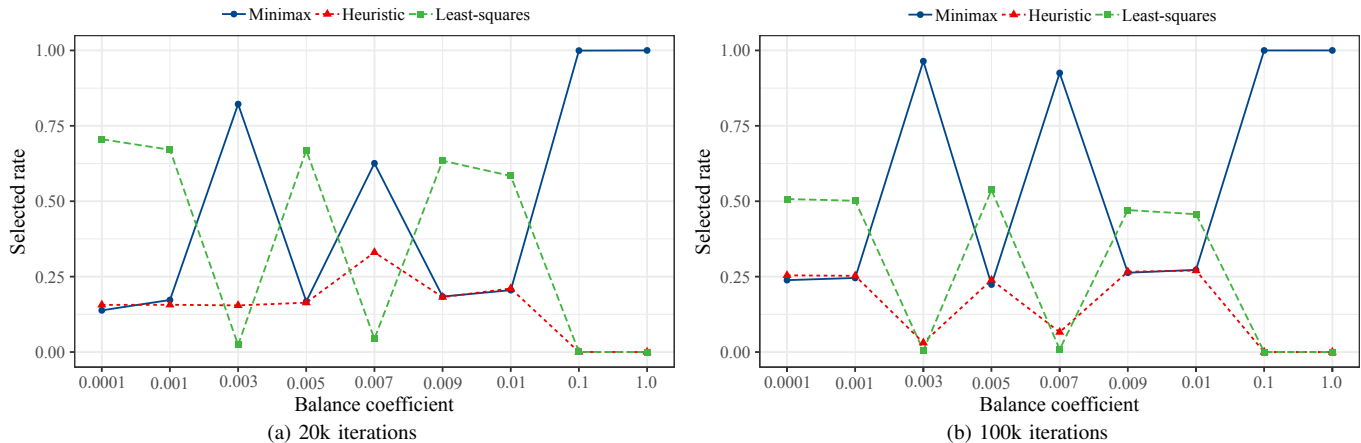


Fig. 11. Selected rate of each operator in E-GANs with various balance coefficient. (a) After training for 20k iterations. (b) After training for 100k iterations.

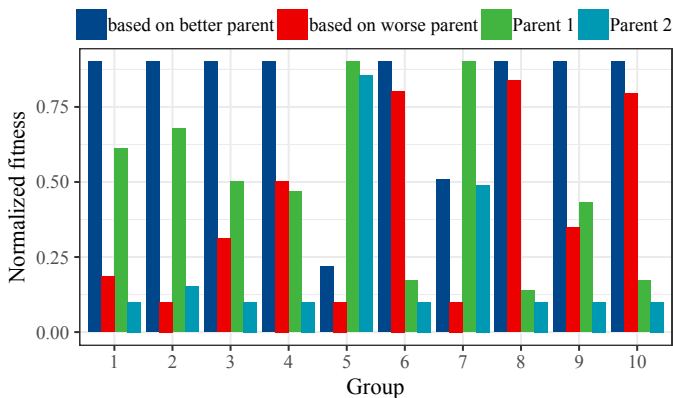


Fig. 12. Normalised crossover performance.

TABLE VII  
FID of Different Crossover Operator.

Methods	Final FID	Best FID
IE-GAN-GP (based on better parent)	<b>24.82</b>	<b>24.82</b>
IE-GAN-GP (based on worse parent)	25.92	25.92

fitness of two parents along with two types of crossover offspring. These values were normalized to  $[0.1, 0.9]$ . Not once did the crossover individual based on worse parent has higher fitness than that based on better parent, and it usually performs worse than better parent or even worse parents. It is difficult to assume that the contribution of the poorer individual can exceed that of the better one.

The results in Table. VII are consistent with expectations. Better operator can help the model to be better trained.

#### H. Validation on More Complex Datasets

To demonstrate that our work can be applied to real-world image datasets, in addition to CIFAR-10 dataset, we also conduct experiments on CelebA dataset with DCGAN network architecture. In the face of this complex dataset, the network architecture is still weak even with the enhanced number of

TABLE VIII  
FID of Different Methods on CelebA over Generator Iteration.

Methods	Best FID
GAN-GP(GAN-Minimax-GP)	56.88
NS-GAN-GP(GAN-Heuristic-GP)	54.58
LSGAN-GP	376.79
GAN-Least-squares-GP	58.01
E-GAN-GP	59.66
(ours) IE-GAN-GP	<b>52.582</b>

channels. To maintain the equilibrium between  $G$  and  $D$ , in this experiment we restrict the discriminator update by setting  $n_D = 1$ .

Six methods are tested: GAN, NS-GAN, LSGAN, GAN-Least-squares, E-GAN and our IE-GAN. Because the discriminator objective functions adopted by IE-GAN are originally used in GAN and NS-GAN, they are just GAN-Minimax and GAN-Heuristic for IE-GAN with  $n_D = 1$ .

The quantitative results are shown in Table. VIII. All methods on this dataset are unstable, so we only compare the best results. The FID value of the real samples is 48.96.

It is clear from the observation that LSGAN essentially fails to be trained, and it is unable to generate meaningful samples. Instead, GAN-Least-squares can be trained, but unlike on CIFAR-10, its performance is the worst among all single mutation operator methods. E-GAN, as always, does not actually benefit from multiple operators and performs the worst among trainable methods. Whereas, our IE-GAN achieves the best results and its score is quite close to that of the true distribution.

It is revealed that IE-GAN can achieve promising results on different datasets, different network architectures, and different operator performances. IE-GAN is not a method specializing for a certain dataset and a certain network architecture. It maintains comparable competitiveness relative to the operators used in various cases.

## VI. CONCLUSION

In this paper, we point out and verify that the evolutionary strategy of E-GAN, especially the diversity fitness function, is unreasonable. We propose a crossover operator that can be widely applied to evolutionary GAN and a more sensible diversity fitness function. We unify them into a universal framework called IE-GAN and implement the framework based on E-GAN. Experiments demonstrate that our approach has better generative performance with less time cost.

## REFERENCES

- [1] I. J. Goodfellow, J. Pouget-Abadie, M. Mirza, B. Xu, D. Warde-Farley, S. Ozair, A. C. Courville, and Y. Bengio, "Generative adversarial nets," in *Proc. NIPS*, Dec. 2014, pp. 2672–2680.
- [2] M. Arjovsky and L. Bottou, "Towards principled methods for training generative adversarial networks," in *Proc. ICLR*, Apr. 2017.
- [3] C. Wang, C. Xu, X. Yao, and D. Tao, "Evolutionary generative adversarial networks," *IEEE Trans. Evol. Comput.*, vol. 23, no. 6, pp. 921–934, 2019.
- [4] S. Chen, W. Wang, B. Xia, X. You, Z. Cao, and W. Ding, "CDE-GAN: cooperative dual evolution based generative adversarial network," *arXiv:2008.09388*, 2020. [Online]. Available: <https://arxiv.org/abs/2008.09388>
- [5] J. Mu, Y. Zhou, S. Cao, Y. Zhang, and Z. Liu, "Enhanced evolutionary generative adversarial networks," in *Proc. CCC*, 2020, pp. 7534–7539.
- [6] M. Baiocchi, C. A. C. Coello, G. D. Bari, and V. Poggioni, "Multi-objective evolutionary GAN," in *Proc. GECCO*, Jul. 2020, pp. 1824–1831.
- [7] J. Toutouh, E. Hemberg, and U. O'Reilly, "Spatial evolutionary generative adversarial networks," in *Proc. GECCO*, Jul. 2019, pp. 472–480.
- [8] Z. Liu, J. Wang, and Z. Liang, "Catgan: Category-aware generative adversarial networks with hierarchical evolutionary learning for category text generation," in *Proc. AAAI*, Feb. 2020, pp. 8425–8432.
- [9] V. Costa, N. Lourenço, J. Correia, and P. Machado, "COEGAN: evaluating the coevolution effect in generative adversarial networks," in *Proc. GECCO*, Jul. 2019, pp. 374–382.
- [10] V. Costa, N. Lourenço, J. Correia, and P. Machado, "Exploring the evolution of gans through quality diversity," in *Proc. GECCO*, Jul. 2020, pp. 297–305.
- [11] B. Rozière, F. Teytaud, V. Hosu, H. Lin, J. Rapin, M. Zameshina, and O. Teytaud, "Evolgan: Evolutionary generative adversarial networks," in *Proc. ACCV*, ser. Lecture Notes in Computer Science, vol. 12625, Nov. 2020, pp. 679–694.
- [12] U. Garciarena, R. Santana, and A. Mendiburu, "Evolved gans for generating pareto set approximations," in *Proc. GECCO*, Jul. 2018, pp. 434–441.
- [13] M. Heusel, H. Ramsauer, T. Unterthiner, B. Nessler, and S. Hochreiter, "Gans trained by a two time-scale update rule converge to a local nash equilibrium," in *Proc. NIPS*, Dec. 2017, pp. 6626–6637.
- [14] J. Li, J. Zhang, X. Gong, and S. Lü, "Evolutionary generative adversarial networks with crossover based knowledge distillation," *arXiv:2101.11186*, 2021. [Online]. Available: <https://arxiv.org/abs/2101.11186>
- [15] G. E. Hinton, O. Vinyals, and J. Dean, "Distilling the knowledge in a neural network," *arXiv:1503.02531*, 2015. [Online]. Available: <http://arxiv.org/abs/1503.02531>
- [16] M. Li, J. Lin, Y. Ding, Z. Liu, J. Zhu, and S. Han, "GAN compression: Efficient architectures for interactive conditional gans," in *Proc. CVPR*, Jun. 2020, pp. 5283–5293.
- [17] A. Aguinaldo, P. Chiang, A. Gain, A. Patil, K. Pearson, and S. Feizi, "Compressing gans using knowledge distillation," *arXiv:1902.00159*, 2019. [Online]. Available: <http://arxiv.org/abs/1902.00159>
- [18] C. Bodnar, B. Day, and P. Lió, "Proximal distilled evolutionary reinforcement learning," in *Proc. AAAI*, Feb. 2020, pp. 3283–3290.
- [19] S. Khadka and K. Tumer, "Evolution-guided policy gradient in reinforcement learning," in *Proc. NeurIPS*, Dec. 2018, pp. 1196–1208.
- [20] I. Gulrajani, F. Ahmed, M. Arjovsky, V. Dumoulin, and A. C. Courville, "Improved training of wasserstein gans," in *Proc. NIPS*, Dec. 2017, pp. 5767–5777.
- [21] M. Arjovsky, S. Chintala, and L. Bottou, "Wasserstein generative adversarial networks," in *Proc. ICML*, ser. Proceedings of Machine Learning Research, vol. 70, Aug. 2017, pp. 214–223.
- [22] A. Jolicœur-Martineau, "The relativistic discriminator: a key element missing from standard GAN," in *Proc. ICLR*, May 2019.
- [23] A. Radford, L. Metz, and S. Chintala, "Unsupervised representation learning with deep convolutional generative adversarial networks," in *Proc. ICLR*, May 2016.
- [24] X. Mao, Q. Li, H. Xie, R. Y. K. Lau, Z. Wang, and S. P. Smolley, "Least squares generative adversarial networks," in *Proc. ICCV*, Oct. 2017, pp. 2813–2821.
- [25] A. Krizhevsky, G. Hinton *et al.*, "Learning multiple layers of features from tiny images," University of Toronto, Tech. Rep., 2009.
- [26] Z. Liu, P. Luo, X. Wang, and X. Tang, "Deep learning face attributes in the wild," in *Proc. ICCV*, Dec. 2015, pp. 3730–3738.
- [27] V. Costa, N. Lourenço, J. Correia, and P. Machado, "Neuroevolution of generative adversarial networks," in *Deep Neural Evolution: Deep Learning with Evolutionary Computation*, H. Iba and N. Noman, Eds. Singapore: Springer Singapore, 2020, pp. 293–322.



**Junjie Li** was born in 1995. He received the B.S. degree in computer science and technology from College of Computer Science and Technology, Jilin University, China, in 2018, and the M.S. degree in computer software and theory from College of Computer Science and Technology, Jilin University, China, in 2021.

His research interests include artificial intelligence and machine learning.



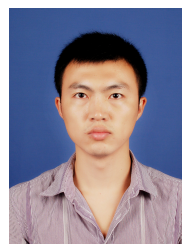
**Jingyao Li** received the B.S. degree in computer science and technology from Jilin University, China, in 2016. She is pursuing the Ph.D. degree in software engineering with Jilin University, China.

Her research interests mainly include transfer learning and domain adaptation. Her email is [jingyao18@mails.jlu.edu.cn](mailto:jingyao18@mails.jlu.edu.cn).



**Wenbo Zhou** received the B.S. degree in computer science and technology from College of Computer Science and Technology, Jilin University, China, in 2014. He received the M.S. and Ph.D. degrees in computer software and theory from Jilin University, China, in 2017 and 2021, respectively. He is a lecture in School of Information Science and Technology, Northeast Normal University, China.

His research interests mainly include formal methods, artificial intelligence, and cloud computing.



**Shuai Lü** received the M.S. and Ph.D. degrees in computer software and theory from Jilin University, China, in 2007 and 2010, respectively, where he is currently an associate professor and Ph.D. supervisor with the College of Computer Science and Technology, Jilin University, China.

His research interests include artificial intelligence, machine learning, and automated reasoning. He has published 115 articles in these areas.